Energy, Mines and Resources Canada
Earth Physics Branch
1 Observatory Crescent
Ottawa Canada
K1A 0Y3

Energie Mines et Ressources Canada
Direction de la physique du globe
1 Place de l'Observatoire
Ottawa Canada
K1A 0Y3

Geothermal Service of Canada

Service géothermique du Canada

HYDRAULIC FRACTURING OF ROCK MASSES. INFLUENCE OF PREEXISTING DISCONTINUITIES. PHASE I.

J.C. Roegiers and T.D. Wiles

Earth Physics Branch Open File No. 81/10

Ottawa, Canada, 1981

31 p.

Price/Prix: $12.35

UNIVERSITY OF TORONTO
Department of Civil Engineering

ISBN 0-7727-7021-2
Publication 81-04

HYDRAULIC FRACTURING OF ROCK MASSES
Influence of preexisting discontinuities
Phase I

J.-C. ROEGIERS
T.D. WILES

APRIL, 1981

Résumé

On discute du comportement de la propagation d'une fracture hydraulique lorsqu'elle se rapproche d'une interface. Afin d'établir une bonne base pour les analyses ultérieures, on fait d'abord la révision du rôle de la mécanique des fractures dans la propagation de fractures hydrauliques.

Le problème d'une interface bimatérielle bien liée est ensuite révisé. On trouve que les analyses exécutées au préalable ne s'appliquent pas. Les principes de la mécanique des fractures sont appliqués de nouveau à ce problème et les résultats ont tendance à être en accord avec le comportement observé.

Le problème d'une interface frictionnelle est analysé. Sous certaines conditions de contraintes on prévoit l'arrêt de la propagation de la fracture. Les résultats en général s'accordent avec le comportement observé.

Abstract

The behaviour of a propagating hydraulic fracture as it approaches an interface is discussed. The role of fracture mechanics in hydraulic fracture propagation is first reviewed to provide a sound basis for further analyses.

The problem of a well bonded bimaterial interface is reviewed and it is found that previously conducted analyses are not applicable. Fracture mechanics principles are reapplied to this problem and results which tend to agree with observed behaviour are found.

The problem of a frictional interface is analysed. It is found that fracture arrest can be expected under certain stress conditions. The results are in general agreement with observed behaviour.

UNIVERSITY OF TORONTO GEOTECHNICAL REPORT

A report prepared for

Energy, Mines & Resources, Canada
Earth Physics Branch,
Ottawa, Ontario.

by

J.-C. Roegiers & T.D. Wiles,
Department of Civil Engineering,
University of Toronto,
Galbraith Building,
Toronto, Ontario.
M5S 1A4.

Contract Number: ISU80-0007

April 1981

FOREWORD

This report constitutes the second and final report on research conducted under contract number ISU80-0007. This report critically reviews previous work and describes some new findings on the topic of hydraulic fracture behaviour in the presence of a preexisting discontinuity. This research has been conducted for the purpose of gaining insight into how to predict hydraulic fracture behaviour in advance of field operations(*).

Any opinions expressed in this report are those of the authors. The Earth Physics Branch takes no responsibility; neither does it endorse the findings.

Toronto, April 1981.

J.-C. Roegiers
T.D. Wiles

(*) The comlementary report published in July 1980 is entitled "Some Applications of the Boundary Integral Technique in Stress Analysis" by T.D. Wiles and J.-C. Roegiers; Reference ISBN 0-7727-7011-5; publication 80-07, Department of Civil Engineering, University of Toronto.

TABLE OF CONTENTS

SUMMARY

The behaviour of a propagating hydraulic fracture as it approaches an interface is discussed. The role of fracture mechanics in hydraulic fracture propagation is first reviewed to provide a sound basis for further analyses.

The problem of a well bonded bimaterial interface is reviewed and it is found that previously conducted analyses are not applicable. Fracture mechanics principles are reapplied to this problem and results which tend to agree with observed behaviour are found.

The problem of a frictional interface is analysed. It is found that fracture arrest can be expected under certain stress conditions. The results are in general agreement with observed behaviour.

NOMENCLATURE

E_i	represents Young's modulus
G	represents the strain energy release rate
K_I	represents the mode I stress intensity factor
ℓ	represents half the fracture length
ℓ_o	represents half the wetted fracture length
p_o	represents fluid pressure acting within the fracture
r	represents distance from the fracture tip
R	represents fracture radius
R_o	represents the wetted fracture radius
u_θ	represents circumferential displacement
v_i	represents Poisson's ratio
x,y	represent co-ordinate axes
σ_θ	represents circumferential stress
$\sigma_1,\sigma_2,\sigma_3$	represent the principal in situ stresses
δ_a,λ,β,w	represent constants
θ	represents an angular co-ordinate
Γ	represents the gamma function
z,ζ,σ_1	represent complex numbers
$\overline{z},\overline{\zeta},\overline{\sigma}_1$	represent conjugate complex numbers
w	represents a mapping function
c	represents half the crack length

c_o	represents half the extent of the pressurized zone
ϕ, ψ	represent analytic stress functions
q_1, q_2	represent field stresses
$\sigma_r, \sigma_\theta, \tau_{r\theta}$	represent respectively the radial, circumferential, and shear stress conponents in the ζ-plane
i	represents an imaginary number
α	represents the inclination of σ_r from σ_x in the z-plane
R	represents the real part
γ, β	represent functions

LIST OF FIGURES

CHAPTER I

INTRODUCTION

The success of hydraulic fracturing operations for secondary recovery of oil and gas or for geothermal energy production depends entirely on the ability to propagate a hydraulic fracture of desired extent. One important consideration in determining the extent of such a man-made frature is its behaviour upon intersection with a preexisting joint, change in material properties, or change in stress state.

The knowledge of the required conditions for fracture impedement or arrest can have an overwhelming influence on the fracture design. If one knew in advance that if more than a given volume of fracturing fluid was injected any additional fluid would be lost in the fracturing of unproductive zones, a pattern of several small fractures may be chosen over a pattern consisting of a few large fractures. In addition, if the influence of pumping pressure and pumping rate on the behaviour of a fracture upon intersection with a joint or discontinuity could be ascertained, more successful fracturing operations could be designed.

To date, only a few field[1-3] and laboratory [4-10] experiments have been conducted to investigate fracture behaviour in discontinuous rock masses. Only a minimal amount of analytical modelling[4,10,11-24] has been conducted and their results show little agreement with the experimentally observed behaviour. It is indicated that either the wrong parameters have been considered, or some very important aspects of the problem have not been considered in the analytical models used.

In this report, the work conducted to date is critically reviewed. The results of analyses incorporating some simple static models are also presented.

CHAPTER II

PROBLEM DESCRIPTION

In order to properly rationalize results, a realistic conception of the problem is necessary. Both analytical[17] and experimental[2,3,25] (laboratory and field) data consistently indicate that hydraulic fractures propagate perpendicular to the minimum principal stress. In addition it is also indicated that unless some external feature such as a discontinuity affects the fracture growth, the fracture tends to be penny-shaped[3,17,26]. Gravitational effects are shown to result in an increased amount of fracture growth in the downward or upward vertical direction depending on the fluid density and the in situ stress gradient, when fractures are oriented in the vertical plane[3,12].

An idealized model of a propagating fracture approaching a discontinuity is illustrated in figure 1. This discontinuity could

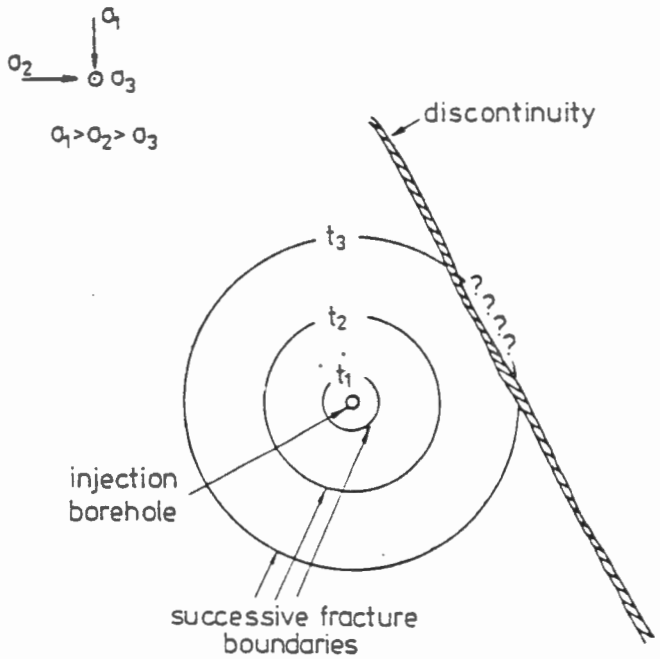

Figure 1 Model of Propagating Hydraulic Fracture

represent a preexisting joint, a fault or an interface between zones with differing material properties or stress states.

For the sake of simplicity it is desirable to conduct two-dimensional analyses whenever possible, but as can be observed in figure 1, until the fracture boundary reaches the discontinuity, no cross-section can be properly analysed assuming plane strain conditions. The use of two-dimensional analyses can therefore, at best, provide qualitative solutions.

If fracture propagation is halted or impeded by intersection with bounding discontinuities, the fracture could take on the elongated shape shown in figure 2. In this case, the assumption of the two-dimensional, plane strain condition is justified in the vicinity of the cross-section indicated.

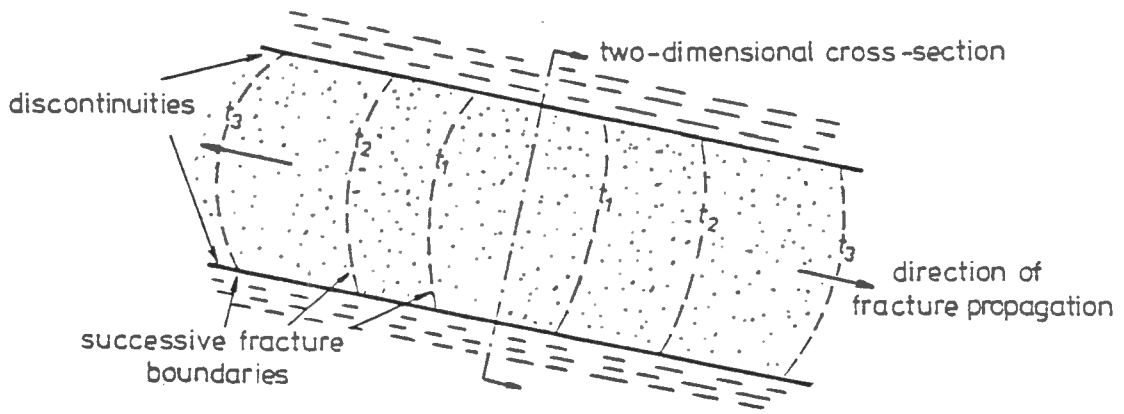

Figure 2 Bounded Hydraulic Fracture

CHAPTER III

ROLE OF FRACTURE MECHANICS IN HYDRAULIC FRACTURE PROPAGATION

Many theoretical arguments used to study the influence of a discontinuity on the propagation of a hydraulic fracture have been based on considerations of the change in the stress intenstiy factor in the vicinity of the discontinuity. In that case, the propagation criterion was simply that the stress intensity at the fracture tip must equal the critical stress intensity factor.

The origins of this fracture criterion go back to a thermodynamic equilibrium theory propsed by Griffith[27,28] which requires that the quantity of strain energy released during fracture propagation be equal to the quantity of energy required to form the new crack surfaces. This criterion requires that the strain energy release rate (where rate refers to change with crack length) be equal to the critical strain energy release rate. By considering the crack tip stress field in a linear elastic, homogeneous medium, this thermodynamic theory was shown to be representable in terms of stress intensity factors[29,31]. The proof depends on the existence of an inverse, root radius singularity in stress at the tip and propagation of the fracture in its own plane (i.e. no curving or branching)[34]. Under the above stated conditions, the stress intensity criterion has been shown to apply (this is reviewed in reference 30).

In hydraulic fracturing, however, consideration must also be given to the fluid flow in the fracture. Fluid mechanics theories

indicate that fracture conductivity depends on the square of the fracture aperture and hence the flow rate depends on the cube of the aperture[32]. Theoretical and experimental investigations have indicated that the fluid cannot penetrate into the narrow tip region of a fracture[4,33]. As a first approximation of this condition a fracture uniformly pressurized over part of its surfaces (see figure 3) was considered.

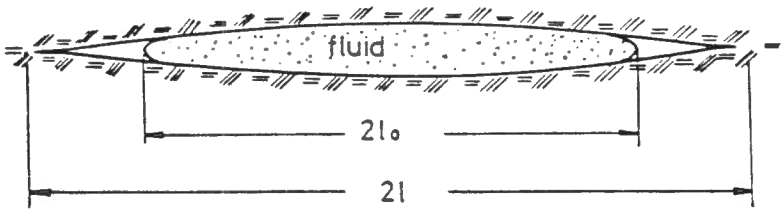

Figure 3 Fracture Pressurized Over Part of its Surface

For the case of a two-dimensional, plane strain fracture the stress intensity factor is given by[30]

$$K_I = 2\, p_o \sqrt{\frac{\ell}{\pi}} \sin^{-1}\left(\frac{\ell_o}{\ell}\right) - \sigma_3 \sqrt{\pi \ell} \quad , \qquad (1)$$

where: p_o represents the pressure in the fracture;

σ_3 represents the minimum principal stress;

ℓ represents one half the fracture length;

ℓ_o represents one half the extent of the pressure distribution.

Similarly for a three-dimensional penny-shaped fracture the result is[30]

$$K_I = \frac{2p_o R_o^2}{\sqrt{\pi} R^{3/2}} \left[1 + \sqrt{1 - \left(\frac{R_o}{R}\right)^2} \right]^{-1} - 2\sigma_3 \sqrt{\frac{R}{\pi}} \quad , \qquad (2)$$

where: R represents the radius of the fracture;

R_o represents the radius of the extent of the pressure distribution.

It can be observed in the expressions that under normal field conditions where the fractures are large and at great depth, the second term on the right hand side of the equations will be so large that the rock strength can be neglected[30]. Even under laboratory conditions where fracture lengths are small and the minimum principal stress is often zero, it has been found that the critical stress intensity factor is small (< 10%) compared to the stress intensity which would result for a uniformly pressurized fracture ($\ell_o=\ell$). The evidence of this statement is the observed large lag of the fluid behind the fracture tip[4].

It is also indicated that under normal field conditions the fracture criterion will be extremely sensitive to the fluid pressure in the fracture. An increase in the fluid pressure by a small percentage of the field stress could increase the stress intensity by a large amount.

CHAPTER IV

FRACTURE PROPAGATION IN A LAYERED MEDIUM WITH DIFFERENT STIFFNESSES AND A WELL-BONDED INTERFACE

Consider the case of fracture approaching a different material (see figure 4a).

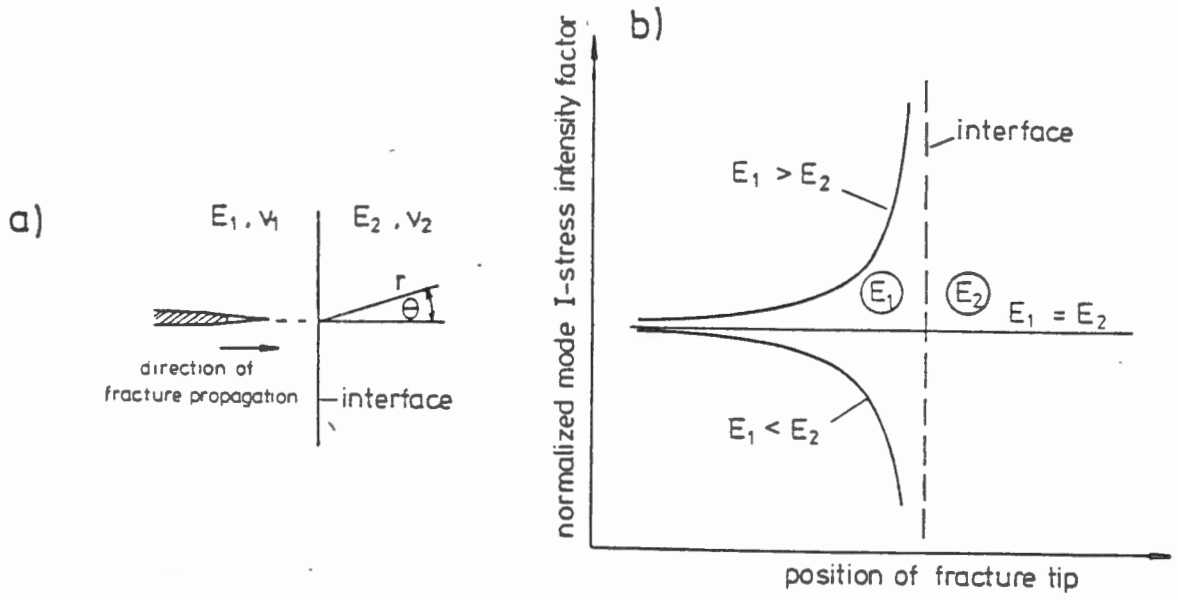

Figure 4 Fracture Propagation in a Layered Medium with Different Stiffnesses
(a) geometry
(b) stress intensity factor near the surface

The stress intensity factor has been calculated for this case[13,19-21] by making the assumptions that:

i) the fracture can be analysed in two dimensions under plane strain, static, elastic conditions;

ii) the entire fracture is uniformly pressurized;

iii) the interface is perfectly bonded;

iv) the fracture is perpendicular to the interface.

The results of the analyses are illustrated in figure 4b. It is indicated that the stress intensity factor decreases to zero when the fracture approaches a stiffer material and that the stress intensity factor increases to infinity when the fracture approaches a less stiff material.

Although one might expect these results to predict that a fracture would be arrested at the interface when approaching a stiffer material, in situ and laboratory experiments have proven that this expectation is false[2-4]. In these experiments, fractures have consistently propagated into materials which are stiffer (in some cases, ten times as stiff).

The reason for this can be explained by consideration of the applicability of the stress intensity fracture criterion in this situation. As has been discussed, the stress intensity approach was derived by assuming an homogeneous medium, a condition which is not satisfied in this problem. Results of analysis also indicate that near the interface the stresses do not exhibit an inverse, root radius variation at the crack tip[13,19-23]. Hence, the stress intensity criterion discussed above does not apply and the results shown in figure 4 do no indicate real fracture behaviour in the vicinity of an interface.

The fundamental strain energy release rate criterion does in fact meet all the required conditions and can be applied in this situation. Using the approach taken by Irwin[29], the strain energy release rate can be determined for the case of a bimaterial interface. The results of previously conducted analysis show that in the immediate vicinity of the crack tip, the stresses and displacements are given by[13,19-21]

(see figure 4a)

$$\sigma_\theta\Big|_{\theta=o} \alpha \quad r^{(\lambda-1)} \quad , \qquad u_\theta\Big|_{\theta=\pi} \alpha \quad r^{\lambda} \quad , \tag{3}$$

where: $\sigma_\theta\Big|_{\theta=0}$ represents the circumferential stress component along the ray oriented at θ equal to zero;

$u_\theta\Big|_{\theta=\pi}$ represents the tangential displacement along the ray oriented at θ equal to π;

λ is a constant depending on the geometry and material properties.

By the same method as used by Irwin[29], the strain energy release rate can be determined as

$$G \alpha \int_0^{\delta a} u_\theta \, (\delta a - r) \, \sigma_\theta \, (r) \, dr \alpha \int_0^{\delta a} (\delta a - r)^{\lambda-1} \, r^{\lambda} \, dr \quad . \tag{4}$$

The integration can be performed by use of the substitution

$$r = \delta a \sin^2 w \quad , \tag{5}$$

giving

$$G \alpha \frac{\Gamma(\lambda+1)\,\Gamma(\lambda)}{\Gamma(2\lambda+1)} \tag{6}$$

where Γ represents the gamma function[36].

The limits on the value of λ are[13,19-23]

$$\lambda = .5 , \tag{7}$$

for a homogeneous material,

$$\lambda = 0 , \tag{8}$$

for intersection of the surface of a semi-infinite medium,

$$\lambda = 1 , \tag{9}$$

for the intersection of a fixed surface.

For other stiffness ratios the value of λ varies between these limits as illustrated in figure 5. The relationship given by equation 6

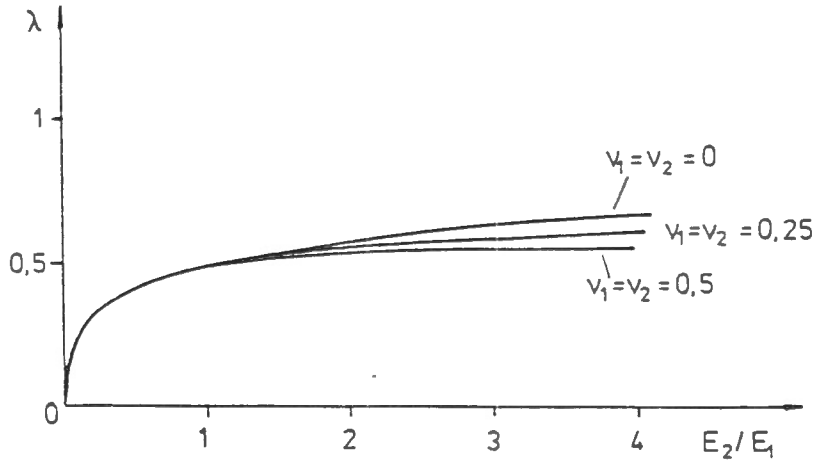

Figure 5

Variation of the constant λ as a function of the Young's moduli ratio

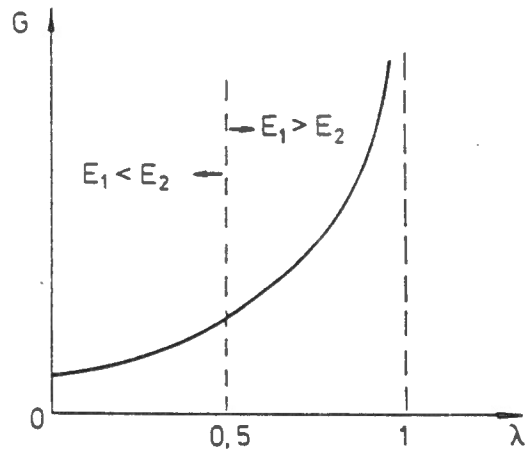

Figure 6 Variation of the Strain Energy Density as a Function of the Constant λ

is illustrated in figure 6. The strain energy release rate can be observed to be finite at the interface, its value dependent on the stiffness ratio.

The result illustrated in figure 6 indicates that there is a tendency for fracture arrest at an interface when approaching a stiffer material. It is thus indicated that an increase in fluid pressure in the fracture should occur upon intersection with a stiffer material. As has been discussed, under field conditions the pressure increase may only be a small percentage of the minimum principal stress and should be more noticeable under laboratory conditions. This type of behaviour has been observed in laboratory experiments[4].

There is a practical limitation on the quantity of fluid flow which can be expected into stiffer layers. Due to the increased stiffness, the fracture apertures are reduced. It is well known that under similar pressure gradients, the fluid flow rate will be extremely sensitive to aperture and hence stiffness. Thus only limited fracture fluid flow should be expected into stiffer layers[14-16,18]. Quantitative results can only be obtained by proper consideration of the actual three-dimensional geometry.

CHAPTER V

FRACTURE PROPAGATION IN A LAYERED MEDIUM WITH DIFFERENT IN SITU STRESSES AND A WELL-BONDED INTERFACE

Consider a fracture tip cross-section propagating in a medium where the minimum principal stress changes abruptly in value from σ_a to σ_b (see figure 7a).

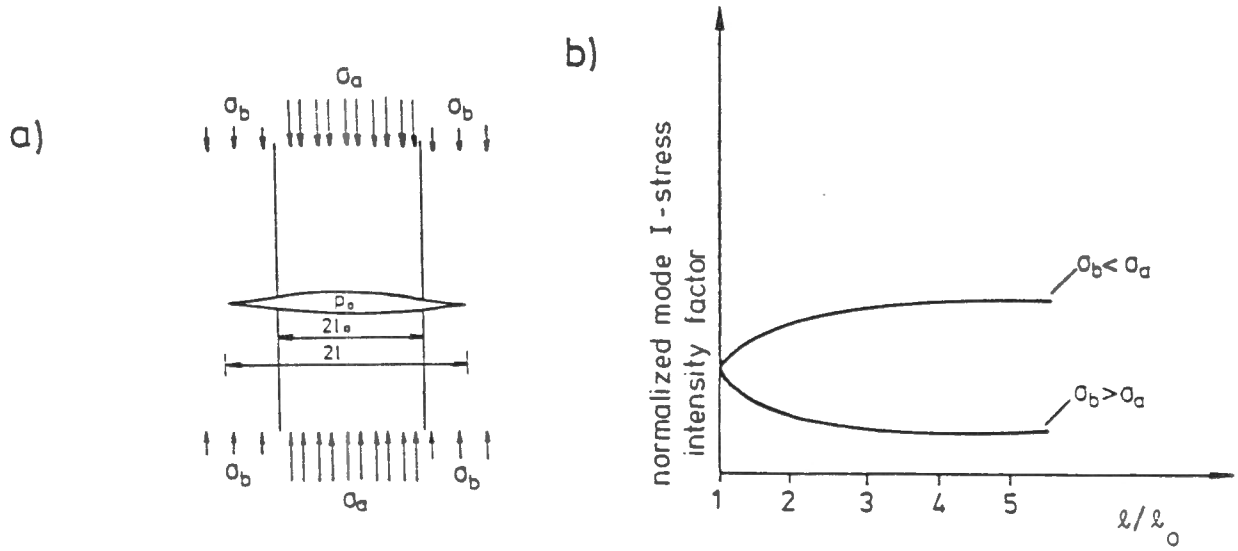

Figure 7 Fracture Propagation in a Layered Medium with Different In Situ Stresses

(a) geometry
(b) stress intensity factor variation

The stress intensity factor has been determined for this case and is given by[12]

$$K_I = 2\,(\sigma_b - \sigma_a)\,\sqrt{\frac{\ell}{\pi}}\,\sin^{-1}\left(\frac{\ell_o}{\ell}\right) + (p_o - \sigma_b)\,\sqrt{\pi\ell} \qquad . \quad (10)$$

This relationship can be plotted and gives the results shown in figure 7b.

It is indicated that the stress intensity factor decreases when the fracture propagates into a zone with a higher, minimum principal stress and the stress intensity factor increases when the fracture approaches a zone with a lower, minimum principal stress. If the minimum principal stress is equal to or exceeds the pressure in the fracture, the stress intensity factor will go to zero.

One might expect these results to predict that a fracture could be arrested at some distance into the higher stress layers. There is experimental evidence which indicates that this is true[3]. In these experiments, fractures propagated only a short distance into higher stressed zones and in some cases there was no penetration.

If fracture propagation were to continue into a higher stressed zone, an increase in fracture fluid pressure would be necessary to maintain the necessary stress intensity at the fracture tip. Equation 10 indicates that the fluid pressure change should be of the order of the in situ stress change.

The practical limits concerning fracture fluid flow into regions of higher or lower minimum principal stress can be arrived at as in the last section. The aperture depends directly on the amount by which the pressure in the fracture exceeds the minimum principal stress. Since the flow rate is very sensitive to the aperture, an increase in the minimum principal stress should be expected to provide a strong limiting influence[14-16,18]. Again, quantitative results can only be obtained by proper modelling of the three-dimensional situation.

CHAPTER VI

FRACTURE PROPAGATION IN A LAYERED MEDIUM WITH A FRICTIONAL INTERFACE

Two sets of independent experiments have been conducted on the influence of preexisting joints on crack arrest[5-10]. The experiments indicate that the likelihood of crack arrest depends on the shear strength of the joint. Lower normal stress or decreased frictional properties are directly related to crack arrest. It is indicated that crack arrest should only be expected when joints are very weak due to shallow operations, clay or gouge fillings[10].

Stress analyses of a fracture approaching a frictional interface in a cube of polymethylmethaclylate have been conducted by one author[10] using photoelastic techniques. His analysis was limited to the case of a fracture perpendicular to the interface, the sample being stressed perpendicular to the interface. It showed that the fracture stopped at the interface for all values of normal interface stress less than 20 MPa. Fracture arrest was associated with a complete lack of transmission of shear stress across the interface.

Experiments have also been conducted on a variety of rock types including limestones and sandstones[5-10]. The loading conditions were the same as stated above. The interface roughness, dampness and time of contact were varied.

The results of the experiments indicate that for each condition considered, there exists a critical normal interface stress associated with fracture arrest. The critical stress can be associated with the

frictional properties in some cases but not in others. It must be noted that the fracture fluid pressure at the time of interface intersection was not considered when analyzing the data.

One set of experiments was conducted on rock samples where the interface surface was coated with montmorillonite[10]. Fracture arrest could not be avoided even under normal interface stresses of 100 MPa.

In order to investigate the governing mechanism of fracture arrest at a frictional interface, extensive two-dimensional analyses of a fracture tip have been conducted. As a first approximation, it has been assumed that the interface does not slip.

The expressions giving the stress field prevailing around a fracture which is uniformly pressurized over part of its surfaces are derived in appendix 1. The normal and shear stress distributions along a line perpendicular to the fracture tip are illustrated in figure 8. These stresses are generated for the specific

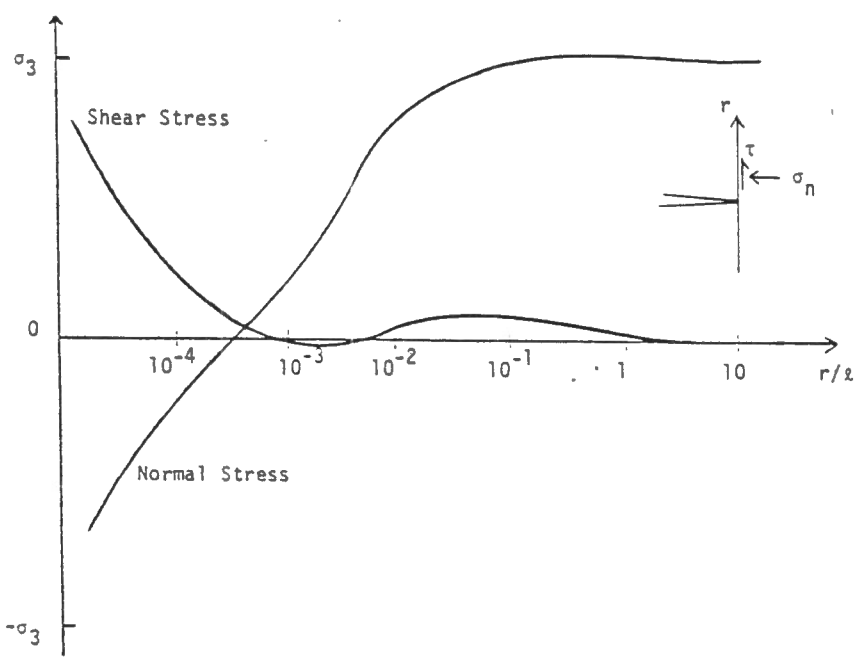

Figure 8 Normal and Shear Stress Distributions

case of

$$p_o = 1.1\ \sigma_3 \quad ,$$
$$K_I = \beta\ p_o\ \sqrt{\pi \ell} = 0.01\ p_o\ \sqrt{\pi \ell} \quad ,$$
$$\frac{\ell_o}{\ell} = .9919 \quad , \qquad (11)$$
$$\sigma_1 = \sigma_3 \quad .$$

The actual amount by which p_o will exceed σ_3 is dependent on the fluid flow conditions and K_{I_C}. The maximum value of K_I which can be assumed for this case is given by

$$K_{I_{MAX}} = (p_o - \sigma_3)\ \sqrt{\pi \ell} = 0.091\ \sqrt{\pi \ell} \quad , \qquad (12)$$

for which case by equation 1

$$\ell_0 = \ell \quad . \qquad (13)$$

It can be observed in figure 8 that there are two regions where shear failure may occur. At very close proximity to the fracture tip, the normal stress becomes negative due to the stress intensity necessary for failure of the rock. At a larger distance from the tip, the shear stress reaches a peak due to the fluid pressurizing the fracture.

It was noted in the photoelastic stress analyses mentioned previously that fracture arrest is usually associated with massive shear slip on the interface. This suggests that the extremely local effects due to the tensile zone around the fracture tip may not be controlling the shear behaviour of the interface; but rather that the

broad shear stress peak due to the fluid pressure in the fracture may have the predominant influence. Thus even though the singularity at the fracture tip may be lost due to local slippage, sufficient force may still be transmitted across the interface to reinitiate fracture growth if massive slip does not occur.

This same situation is better illustrated in figure 9 where the ratio of the shear stress to normal stress is plotted for several stress intensity values. As discussed before, the value of β ranges from near zero to a small fraction (< 10%) of its maximum value.

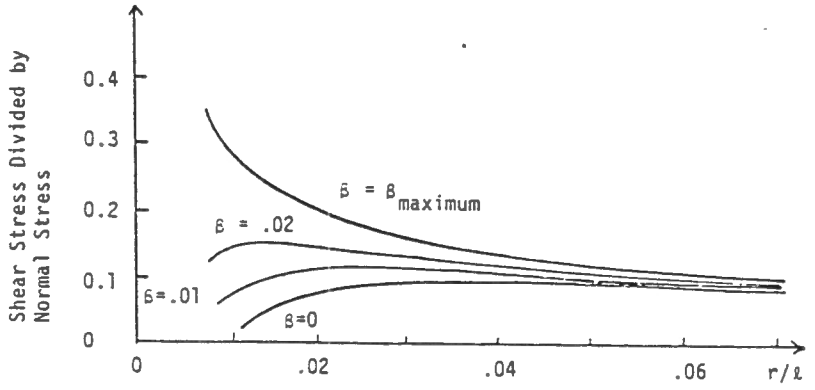

Figure 9 Shear Stress Ratio for Several Values of Stress Intensity

Finally, in figure 10 the maximum value of shear stress over normal stress is plotted under a variety of conditions assuming that β is equal to zero. It can be observed that the shear failure should be difficult to prevent if the shear strength is very small. This condition could result due to joint infilling with clay or gouge, or due to the use of laboratory materials which exhibit very low frictional properties such as smooth plastics.

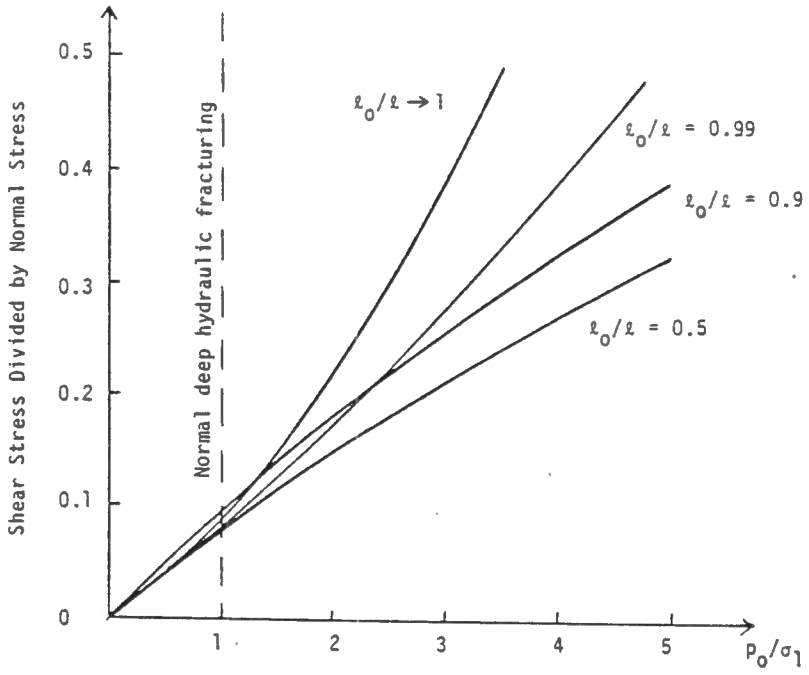

Figure 10 Maximum Shear Stress Ratio for Various Stress States

Hydraulic fracturing in deep formations with low viscosity fracturing fluids implies that the pressure in the fracture should be only slightly larger than the minimum principal stress and that[32]

$$\ell_0/\ell \to 1 \ . \tag{14}$$

Under these conditions the maximum principal stress will normally exceed the fluid pressure in the fracture. The line indicating normal deep hydraulic fracturing is drawn based on this reasoning.

It is indicated that for this case, shear failure should not be expected. If highly viscous fracturing fluids are used, or if a weak joint or fault is intersected, fracture arrest may occur.

Figure 9 also indicates that high fluid pressure and low in situ stresses can be associated with fracture arrest at joint intersections. The apparent sensitivity of the results to the magnitude of ℓ_o indicates that the results are sensitive to the pressure distribution in the fracture. For higher fluid pressures, analysis incorporating more realistic fluid pressure distributions may be required.

CHAPTER VII

CONCLUSIONS

Although detailed experimental and analytical work is necessary to quantify the results indicated in this report, the results do show strong trends. There is sufficient agreement between the analysis and experimental work presented to indicate that the governing mechanisms discussed are correct.

The results of previous analyses concerning the behaviour of the stress intensity factor in the vicinity of a bimaterial interface do not properly indicate the real fracture behaviour. This is due to the fact that the stress intensity criterion does not apply in this particular case. New results have been presented based on the more fundamental strain energy release rate criterion. These results show agreement with experimental data.

It is indicated that a rise in fracture fluid pressure is necessary in order to propagate a fracture across a well bonded interface into a stiffer zone. Practical limitations show that only a limited quantity of fluid can flow into these stiffer zones.

Since higher fluid pressures are associated with higher pumping rates, both of these can be expected to lead to increased fracture propagation into stiffer zones.

Experimental and analytical results both indicate that higher stress layers tend to suppress fracture propagation. If the stress in a bounding layer exceeds the fracture fluid pressure, the layer must act as a barrier.

A rise in fracture fluid pressure can be associated with propagation into a higher stress layer. Fluid flow will however be limited due to the expected reduction in fracture aperture.

Higher fluid pressures and thus higher pumping rate can be expected to lead to increased fracture propagations into higher stress zones.

In both the cases of a bimaterial interface and changing in situ stresses, three-dimensional analysis of fracture fluid flow can only lead to correct statements concerning the quantities of fluid loss into bounding layers.

It has been shown that a frictional interface can provide a barrier to fracture propagation. Fracture arrest is not likely to occur on clean joints at great depth when using low viscosity fracturing fluids. However, for any other conditions than these it is shown that fracture arrest may occur.

There is a paricularly strong tendency for fracture arrest at a frictional interface under the following conditions:

i) Low shear strength joints due to clay or gouge infilling, or the use of low shear strength materials in laboratory experiments tend to increase the possibility of fracture arrest.

ii) Increased fracture fluid pressures tend to increase the likelihood of fracture arrest provided the percentage of wetted area remains constant. There is a particularly sharp increase for values of fracture fluid pressure which exceeds the in situ stress normal to the joint.

Fracture mechanics arguments have been applied to all three aspects considered of the fracture interface problem. These arguments have lead to plausable explanations of the observed phenomena and have thus also indicated the direction for future work. Most of the results presented in this discussion have been based on laboratory scale experiments and two-dimensional approximations. The accuracy of these results can only be assessed by more rigorous three-dimensional analysis and full scale monitoring of hydraulic fracture operations.

REFERENCES

1. Warpinski, N.R., Schmidt, R.A., Northrop, D.A., and Tyler, L.D., "Hydraulic Fracture Behaviour at a Geologic Formation Interface: Pre-Mineback Report", U.S. Government Report SAND78-1578, October, 1978.

2. Northrop, D.A., Warpinski, N.R., and Schmidt, R.A., "EGR Stimulation Research Project - Direct Observation of Hydraulic and Dynamic Fracturing", U.S. Government Report De-AC04-70P00789.

3. Warpinski, N.R., Schmidt, R.A., and Northrop, D.A., "In Situ Stresses: The Predominant Influence on Hydraulic Fracture Containment", Soc. Pet. Eng. 8932, 1980.

4. Daneshy, A.A., "Hydraulic Fracture Propagation in Layered Formations", Soc. Pet. Eng. Journal, Feb. 1978.

5. Shaffer, R.J., Hanson, M.E., Anderson, G.O., "Hydraulic Fracturing Near Interfaces", U.S. Government Reports, UCRL-83419, September 1979.

6. Anderson, G.D., "Effects of Mechanical and Frictional Rock Properties on Hydraulic Fracture Growth Near Unbonded Interfaces", U.S. Government Report, UCRL-82456, July 1979.

7. Hanson, M.E., Anderson, G.D., Shaffer, R.J., "Theoretical and Experimental Analyses of Hydraulic Fracturing and Some Reservoir Response to the Stimulation", U.S. Government Report, UCRL-82578, 1979.

8. Anderson, G.O., Larson, D.B., "Laboratory Experiments on Hydraulic Fracture Growth Near an Interface", U.S. Government Report, UCRL-80355, 1979.

9. Hanson, M.E., Anderson, G.D., and Shaffer, R.J., "Theoretical and Experimental Research on Hydraulic Fracturing", U.S. Government Report, UCRL-80558, 1978.

10. Teufel, L.W., An Experimental Study of Hydraulic Fracture Propagation In Layered Rock, Ph.D. Thesis, Texas A & M University, 1979.

11. Advani, S.H., "Finite Element Model Stimulations Associated with Hydraulic Fracturing", Soc. Pet. Eng. 8941, 1980.

12. Simonson, E.R., Abou-Sayed, A.S., Clifton, R.J., "Containment of Massive Hydraulic Fractures", Soc. Pet. Eng. Journal, Feb. 1978.

13. Hanson, M.E., Shaffer, R.J., "Some Results from Continuum Mechanics Analyses of the Hydraulic Fracturing Process", Soc. Pet. Eng. Journal, April, 1980.

14. Cleary, M.P., "Analysis of Mechanisms and Procedures for Producing Favourable Shapes of Hydraulic Fractures", Soc. Pet. Eng. 9260, 1980.

15. Cleary, M.P., "Primary Factors Governing Hydraulic Fractures in Heterogeneous Stratified Porous Formations", Energy Technology Conference and Exhibition, Houston, Texas, November 1978.

16. Cleary, M.P., "Rate and Structure Sensitivity in Hydraulic Fracturing of Fluid-Saturated Porous Formations", 20th U.S. Symposium on Rock Mechanics, Austin, Texas, 1979.

17. Chang, H.Y., "Development of Improved Design Criteria for Hydraulic Fracturing Operations", Ph.D. Thesis, West Virginia University, 1978.

18. Van Elken, H., "Hydraulic Fracture Geometry: Fracture Containment in Layered Formation", Soc. Pet. Eng. 9261, 1980.

19. Ashbaugh, N.E., "Stresses in Laminated Composites Containing a Broken Layer", Journal of Applied Mechanics, p. 533, V 40, 1978.

20. Cook, T.S. and Erdogan, F., "Stress in Bonded Materials with a Crack Perpendicular to the Interface", International Journal Eng. Sc., p. 677, V 10, 1972.

21. Erdogan, F. and Biricikoglu, V., "Two Bonded Half Planes with a Crack Going Through the Interface", Int. Journal Eng., Sci., p. 745, F 11, 1973.

22. Goree, J.G. and Venezia, W.A., "Bonded Elastic Half-planes with an Interface Crack and a Perpendicular Intersecting Crack that Extends Into the Adjacent Material - I", Int. Journal Eng. Sci., p. 1, V 15, 1977.

23. Goree, J.G., and Venezia, W.A., "Bonded Elastic Half-Planes with an Interface Crack and a Perpendicular Intersecting Crack that Extends into the Adjacent Material - II", Int. Journal Eng. Sc., p. 19, V 15, 1977.

24. Abe, H., Mura, T. and Keer, L.M., "Growth Rate of a Penny-Shaped Crack in Hydraulic Fracturing of Rocks", Journal of Geophysical Research, V 81, No. 29, 1976.

25. Daneshy, A.A., "A Study of Inclined Hydraulic Fractures", Soc. Pet. Eng. Journal, p. 61, April 1973.

26. Mastojannis, E.N., Keer, L.M., and Mura, T., "Growth of Planar Cracks Produced by Hydraulic Fracturing", Int. Journal Num. Methods, p. 41, V 15, 1980.

27. Griffith, A.A., "The Phenomena of Rupture and Flow in Solids", Phil. Trans, Royal Society London, p. 163, V A221, 1921.

28. Griffith, A.A., "The Theory of Rupture", Proc. Int. Cong. Appl. Mech., 1924.

29. Irwin, G.R., "Analysis of Stresses and Strains Near the Edge of a Crack Traversing a Plate", Trans. Am. Soc. Mech. Eng., Journal Applied Mech.

30. Barenblatt, G.I., "The Mathematical Theory of Equilibrium Cracks in Brittle Fracture", Advances in Applied Mechanics, p. 55, V 7, 1962.

31. Irwin, G.R., "Relation of Stresses Near a Crack to the Crack Extension Force", Proc. 9th Int. Cong. Appl. Mech., Brussels, P. 245, 1957.

32. Streeter, V.L., Fluid Mechanics, McGraw Hill Book Co., 1971.

33. Khristianovic, S.A. and Zheltov, Y.P., "Formation of Vertical Fractures by Means of Highly Viscous Fluid", Proc. 4th World Pet. Cong. p. 579, V 2, 1955.

34. Liebowitz, H. (Ed.), Fracture - An Advanced Treatise, VII, Academic Press, New York, 1968.

35. Hanson, M.E., Anderson, G.D. and Shaffer, R.J., "Effects of Various Parameters on Hydraulic Fracture Geometry", U.S. Government Report, UCRL - 83784, May 1980.

36. Abramowitz, M. and Stegun, I., Handbook of Mathematical Functions, Dover Publications Inc., New York, 1970.

37. Muskhelishvili, N.I., Some Basic Problems of the Mathematical Theory of Elasticity, Groningen, Netherlands, 1963.

APPENDIX - STRESS AROUND A PART PRESSURIZED FRACTURE IN A BIAXIAL STRESS FIELD

The stress in the vicinity of a part pressurized, two dimensional, flat elliptic crack can be generated by the use of complex analytic stress functions. The geometry and coordinate system are illustrated in figure 11.

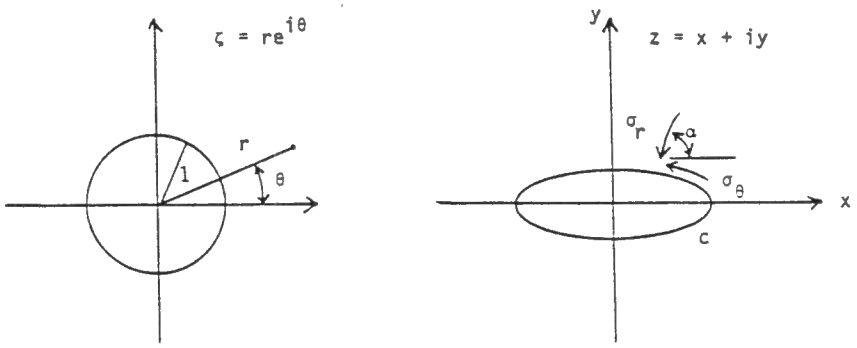

Figure 11 Geometry and Coordinate System

The mapping function considered is given by

$$z = w(\zeta) = \frac{c}{2}\left(\zeta + \frac{1}{\zeta}\right) \quad ,$$

where: z represents the complex variable in the x-y coordinate plane,

ζ represents the complex variable in the r-θ coordinate plane;

w represents a mapping function;

c represents one half the fracture length.

The function maps a flat elliptic crack of length 2c in the x-y plane, onto a circle of unit radius in the r-θ plane.

This function gives the relations

$$x = \frac{c}{2}\left(r + \frac{1}{r}\right)\cos\theta \quad ,$$

$$y = \frac{c}{2}\left(r - \frac{1}{r}\right)\sin\theta \quad .$$

The required loading conditions are illustrated in figure 12.

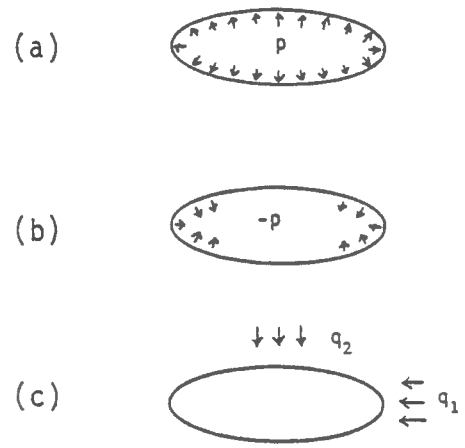

Figure 12 Loading Conditions

The stress functions for each case illustrated in figure 12 a, b, c are given by

$$\phi_a = -\frac{pc}{2\zeta} \quad ,$$

$$\psi_a = -\frac{pc\,\zeta}{(\zeta^2-1)} \quad ,$$

$$\phi_b = \frac{pc}{4\pi i}\left[\frac{4}{\zeta}\,\ell n\,\sigma_1 - \left(\zeta + \frac{1}{\zeta}\right)\ell n\left(\frac{\zeta^2-\sigma_1^2}{\zeta^2-\bar{\sigma}_1^2}\right) - \left(\sigma_1 + \frac{1}{\sigma_1}\right)\ell n\left(\frac{\zeta+\sigma_1}{\zeta-\sigma_1}\cdot\frac{\zeta-\bar{\sigma}_1}{\zeta+\bar{\sigma}_1}\right)\right]$$

$$\psi_b = \frac{pc}{4\pi i}\left[\frac{8\zeta}{(\zeta^2-1)}\,\ell n\,\sigma_1 - \left(\sigma_1 + \frac{1}{\sigma_1}\right)\,n\left(\frac{\zeta+\sigma_1}{\zeta-\sigma_1}\cdot\frac{\zeta-\bar{\sigma}_1}{\zeta+\bar{\sigma}_1}\right)\right] ,$$

$$\phi_c = \frac{-(q_1+q_2)}{8}\,c\,\left(\zeta + \frac{1}{\zeta}\right) + \frac{q_2\,c}{2\zeta} ,$$

$$\psi_c = \frac{(q_1-q_2)\,c}{4}\,\left(\zeta + \frac{1}{\zeta}\right) + \frac{q_2\,c\zeta}{(\zeta^2-1)} ,$$

where: ϕ,ψ represent a pair of stress functions;

p represents the pressure in the fracture;

q_1, q_2 represent the field stresses.

In these expressions the extent of the pressurized portion of the fracture surface is represented in the x-y plane by $2c_o$ and in the r-θ plane by σ_1 where

$$\sigma_1 = e^{i\theta_o} ,$$

$$\bar{\sigma}_1 = e^{-i\theta_o} ,$$

$$c_o = \cos\,\theta_o .$$

The stresses can be determined by superimposing these stress functions and substituting into

$$\sigma_r + \sigma_\theta = 2\left(\frac{\partial\phi}{\partial z} + \overline{\frac{\partial\phi}{\partial z}}\right) \quad ,$$

$$\sigma_\theta - \sigma_r + 2i\,\tau_{r\theta} = \left(2\overline{z}\,\frac{\partial^2\phi}{\partial z^2} + 2\,\frac{\partial\psi}{\partial z}\right) e^{2i\alpha} \quad ,$$

$$\tan\alpha = \frac{\partial y}{\partial x} = \left(\frac{r^2+1}{r^2-1}\right)\tan\theta \quad ,$$

where: $\sigma_r, \sigma_\theta, \tau_{r\theta}$ represent respectively the radial, circumferential and shear stress components;

α represents the inclination of the radial stress component from the x-axis.

The resulting stresses are given by

$$\gamma^{-1} = (\zeta^2 - 1)(\overline{\zeta}^2 - 1) = r^4 - 2r^2\cos 2\theta + 1$$

$$\sigma_r + \sigma_\theta = -q_1 - q_2 + 2\left[p\left(1 - \frac{2\theta_o}{\pi}\right) - q_2\right]\left[\frac{1}{(\zeta^2-1)} + \frac{1}{(\overline{\zeta}^2-1)}\right]$$

$$+ R\left[\frac{2pi}{\pi}\,\ell n\left(\frac{r^2 - e^{2i(\theta_o-\theta)}}{r^2 - e^{-2i(\theta_o+\theta)}}\right)\right]$$

$$= -q_1 - q_2 + 4\left[p\left(1 - \frac{2\theta_o}{\pi}\right) - q_2\right]\gamma\,(r^2\cos 2\theta - 1)$$

$$+ \frac{2p}{\pi}\left\{\tan^{-1}\left[\frac{\sin 2(\theta_o-\theta)}{r^2 - \cos 2(\theta_o-\theta)}\right] + \tan^{-1}\left[\frac{\sin 2(\theta_o+\theta)}{r^2 - \cos 2(\theta_o+\theta)}\right]\right\}$$

$$\sigma_\theta - \sigma_r + 2i\tau_{r\theta} = -4\gamma^2 \left[p\,(1-\frac{2\theta_o}{\pi}) - q_2 \right] \left[\zeta^2\,(\bar{\zeta}^4-1) - \zeta\bar{\zeta}\,(\zeta^2+1)(\bar{\zeta}^2-1) \right]$$

$$+ (q_1 - q_2)\,\gamma\,\bar{\zeta}^2\,(\zeta^2 - 1)^2/\zeta\bar{\zeta}$$

$$+ \frac{2pi}{\pi}\,\gamma\alpha\,(\zeta^2-1)(\sigma_1^2-\bar{\sigma}_1^2)\left[\zeta^2(\bar{\zeta}^2+1) - \zeta\bar{\zeta}(\zeta^2+1)\right]\,(\bar{\zeta}^2-\bar{\sigma}_1^2)(\bar{\zeta}^2-\sigma_1^2)$$

$$= -4r^2\,\gamma^2\,(r^4 - 1)\,(\cos2\theta - 1)\left[p\,(1 - \frac{2\theta_o}{\pi}) - q_2\right]$$

$$+ (q_1 - q_2)\,\gamma\left[(r^4 + 1)\cos2\theta - 2r^2\right]$$

$$+ 2i\,\{2r^2\,\gamma^2(r^2 - 1)^2 \sin2\theta\left[p(1 - \frac{2\theta_o}{\pi}) - q_2\right]$$

$$+ \frac{(q_1 - q_2)}{2}\,\gamma\,(r^4 - 1)\,\sin2\theta\,\}$$

$$+ \frac{4p}{\pi}\,\gamma\alpha r^2\,(r^2-1)\,\sin2\theta_o\,(\cos2\theta-1+i\,\sin2\theta)(r^2\cos2\theta-1+ir^2\sin2\theta)$$

$$\times\left[r^4\,\cos4\theta - 2r^2\,\cos2\theta\,\cos2\theta_o + 1\right.$$

$$\left.-i\,(r^4\,\sin4\theta - 2r^2\,\sin2\theta\,\cos2\theta_o)\right]$$

$$\alpha^{-1} = (\zeta^2 - \sigma_1^2)\,(\zeta^2 - \bar{\sigma}_1^2)\,(\bar{\zeta}^2 - \bar{\sigma}_1^2)(\bar{\zeta}^2 - \sigma_1^2)$$

$$= \left[r^4 - 2r^2\cos\,2(\theta_o - \theta) + 1\right]\left[r^4 - 2r^2\,\cos2(\theta_o + \theta) + 1\right]$$

These expressions can be easily evaluated with the aid of a programmable calculator. The stresses given by these relations are illustrated in figure 8.